

AMMONIA DISPERSION FROM MULTI-FLOOR VERSUS STANDARD SINGLE-FLOOR PIG PRODUCTION FACILITIES BASED ON COMPUTATIONAL FLUID DYNAMICS SIMULATIONS

Yicong XIN¹, Li RONG², Gunther SCHAUBERGER³, Dejie LIU¹, Xiusong LI⁴, Zhihua YANG⁵, Songming ZHU¹, Dezhao LIU (✉)¹

- 1 Key Laboratory of Equipment and Informatization in Environment Controlled Agriculture, Ministry of Agriculture and Rural Affairs, Key Laboratory of Intelligent Equipment and Robotics for Agriculture of Zhejiang Province, Institute of Agricultural Bio-Environmental Engineering, College of Biosystems Engineering and Food Science, Zhejiang University, Hangzhou 310058, China.
- 2 Department of Civil and Architectural Engineering—Building Science, Aarhus University, Aarhus C 8000, Denmark.
- 3 WG Environmental Health, Unit for Physiology and Biophysics, University of Veterinary Medicine, A-1210 Vienna, Austria.
- 4 Big Herdsman Machinery Co., Ltd., Qingdao 266000, China.
- 5 Zhejiang Huatong Meat Products Co., Ltd., Yiwu 322000, China.

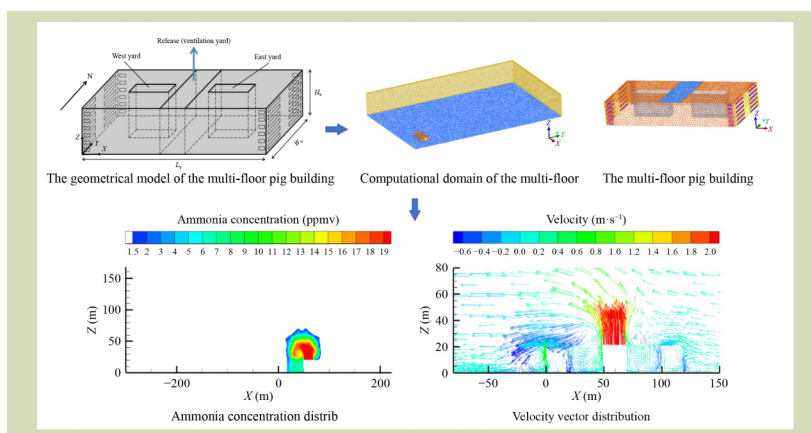
KEYWORDS

pig building, computational fluid dynamics, ammonia, dispersion

HIGHLIGHTS

- NH₃ dispersion from a multi-floor pig building was compared to a single-floor building.
- NH₃ dispersed much further from the multi-floor pig building.
- Wind speed, direction and source concentration were important for NH₃ dispersion.
- NH₃ tended to accumulate in the east and west yards of the multi-floor pig building.
- Higher wind speed was the likely cause of more NH₃ accumulation in the yards.

GRAPHICAL ABSTRACT



ABSTRACT

Multi-floor buildings for raising pigs have recently attracted widespread attention as an emerging form of intensive livestock production especially in eastern China, due to the fact that they can feed a much larger number of animals per unit area of land and thus alleviate the shortage of land available for standard single-floor pig production facilities. However, this more intensive kind of pig building will pose new challenges to the local environment in terms of pollutant dispersion. To compare the dispersion air pollutants (ammonia as a representative) emitted from multi- versus single-floor pig buildings, ammonia dispersion distance and concentration gradients were investigated through three-dimensional simulations based on computational fluid

Received December 30, 2022;

Accepted April 14, 2023.

Correspondence: dezhao_l@163.com

dynamics. The validation of an isolated cubic model was made to ensure the simulation method was effective. The effects of wind direction, wind speed and emission source concentration at 1.5 m (approximate human inhalation height) during summer were investigated. The results showed that the ammonia dispersion distance of the multi-floor pig building was far greater than that of the single-floor building on a plane of $Z = 1.5$ m. When the wind direction was 67.5° , the wind speed was $2 \text{ m}\cdot\text{s}^{-1}$ and the emission source concentration was 20 ppmv, the dispersion distance of the multi-floor pig building could reach 1380 m. Meanwhile, the ammonia could accumulate in the yard to 7.68 ppmv. Therefore, future site selection, wind speed and source concentration need to be given serious consideration. Based on the simulation used in this study with source concentration is 20 ppmv, the multi-floor pig buildings should be located 1.4 km away from residential areas to avoid affecting residents. The results of this study should guidance for any future development of multi-floor pig buildings.

© The Author(s) 2023. Published by Higher Education Press. This is an open access article under the CC BY license (<http://creativecommons.org/licenses/by/4.0>)

1 INTRODUCTION

Over recent decades, China has become the largest market in the world for meat products as living standards have unceasingly increased and the demand for meat has had high rates of growth^[1]. In 2021, total meat consumption in China reached nearly 100 Mt, accounting for 27% of the global total (according to the reports by McKinney & Company). Consequently, animal production in China has been expanding significantly^[2]. However, the standard production modes in the Chinese livestock industry have not keep up with the increasing demand for meat supply. The livestock industry has moved rapidly toward modernization and intensification.

The number of intensive livestock production facilities has increased rapidly with this intensification of the industry. However, the construction of intensive production facilities requires large areas of high-quality land, and the shortage of available land has become a main obstacle to further intensification of the livestock production in China. Therefore, in recent years, the developed multi-floor buildings for producing pigs has become an attractive and popular option in the emerging mode of intensive livestock production. By making use of vertical space, the multi-floor pig buildings can greatly save land by increasing production per unit area of land. Also, with the height difference between floors there are benefits for combined waste disposal. However, the adoption of multi-floor pig buildings in China has been rapid and without detailed research on the potential environmental impacts, such as dispersal of air pollutants.

Considerable quantities of ammonia are released during pig production and this will be more concentrated when using multi-floor buildings. Ammonia is considered to be a marker for livestock-related air pollution and from agricultural sources it represents about 80%–90% of total anthropogenic emissions^[3]. Ammonia can travel great distances which substantially contributes to the ambient concentration of $\text{PM}_{2.5}$ and it can react with atmospheric acids to form ammonium^[4,5]. The dispersion of ammonia negatively affects the ambient air quality and increases the incidence of human respiratory diseases^[6,7]. In addition, complaints about the nuisance caused by odors from livestock production facilities have increased in recent years and previous studies have shown that ammonia was considered one of the main components of odor^[8]. Therefore, it is imperative to investigate the ammonia dispersion from multi-floor pig buildings to provide guidance for their increasingly widespread adoption, as there appears to be no currently published studies comparing pollutants emitted from multi- versus single-floor pig buildings.

However, airflow in the atmospheric boundary layer above buildings is inherently complex. It is therefore difficult to obtain an adequate amount of empirical data of sufficient precision to determine how to control atmospheric air movement^[9]. The computational fluid dynamics (CFD) approach, which provides the information of the distribution of several parameters (e.g., air speed, temperature, humidity and concentration) around buildings with complex geometric shapes at every point in the computational domain, has been increasingly used for the analysis of urban microclimate^[10–14]. Also, CFD has been applied to the modeling of dispersion of air

pollutants (e.g., carbon dioxide and ammonia) in street canyons and urban geometry. Gu et al.^[15] used CFD to investigate the influence of vegetation canopy layer and atmospheric conditions on airflow and pollutant distribution in a street canyon by using large eddy simulation. Tan et al.^[16] used CFD to study the influence of the diurnal variation of surface temperature on airflow patterns and pollutant dispersion in the street canyon under varying thermal stratification. Olivardia et al.^[17] used CFD analysis of airflow patterns and pollutant dispersion in a realistic urban canyon for over 24 h. These studies show that CFD is an economical and promising tool to study the dispersion of pollutants in a context with multi- and single-floor buildings.

Overall, this study aimed to conduct three-dimensional CFD simulations based on the actual dimensions of representative multi- and single-floor pig buildings with ammonia as the target gas. This simulation was done for summer due to the increased ventilation rate and potential dispersion distance in summer. The objectives of this study were to use CFD analysis to (1) investigate the difference of ammonia dispersion between a representative multi- and single-floor pig buildings; (2) evaluate the effects of wind direction, wind speed and ammonia emission source concentration on the ammonia dispersion; and (3) analyze the ammonia dispersion distance from a multi-floor pig building.

2 MATERIALS AND METHODS

2.1 Validation of simulation method

Many generic studies which focused on simplified configuration, such as isolated buildings, have proven to be suitable for validation^[11], since the complex flow and dispersion processes and other salient features in the complex real environment are also contained in the simplified situation. Additionally, the simulation methods can be used in both generic and applied contexts^[18,19]. In this study, the wind-tunnel measurements^[20] were used for validation. The experiment measured the velocity and concentration around an isolated cubic model building with $H_b = 0.05$ m within the neutral surface boundary layer. The geometrical model is shown in Fig. 1. Pure helium as a tracer gas was released from a circular center rooftop vent. The CFD simulation was conducted based on the experiment and the simulation of velocity and pure helium concentration were compared with the experimental results. The realizable $k-\epsilon$ turbulence model and scalable wall function were used. For the grid sensitivity analysis, the computational domain was discretized into

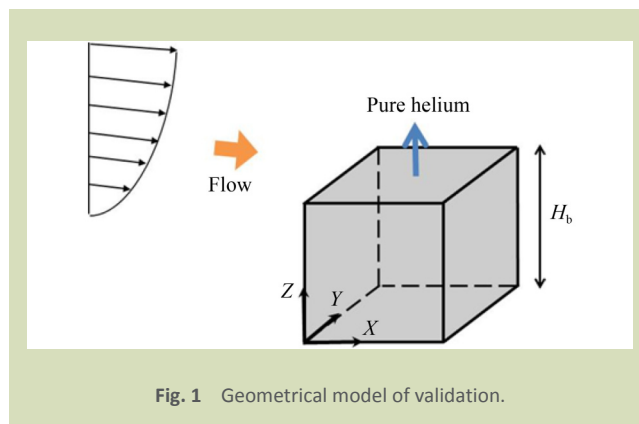


Fig. 1 Geometrical model of validation.

1,680,763, 2,844,807 and 5,088,346 computational grids for the coarse, medium and fine grids, respectively. Eventually, the medium grid was adopted in this study considering the cost of the calculation.

2.2 CFD modeling

2.2.1 Geometrical model

The selected multi-floor pig building (Fig. 2) was located in Yiwu, Zhejiang Province, China (29°21' N, 119°94' E). It had six floors containing 24 pig houses and each pig house could raise 1000 pigs. The length, width and height of the building were 118, 62 and 21 m, respectively, and the floor space of the multi-floor building was 7316 m². The building was symmetric and there was a ventilation yard with an area of 1240 m² in the center of the building which was the only gas emission outlet. Ninety-six VX51 fans (Munters Air Treatment (Beijing) Co., Ltd., Beijing, China) with a ventilation rate of $\sim 47,000$ m³·h⁻¹ and 48 VX24 fans (Munters Air Treatment (Beijing) Co., Ltd., Beijing, China) with a ventilation rate of 9945 m³·h⁻¹ were installed at both sides of the ventilation yard. There was also a yard with windows on the east and the west sides of the building. For each pig house, six wet pads were installed at the

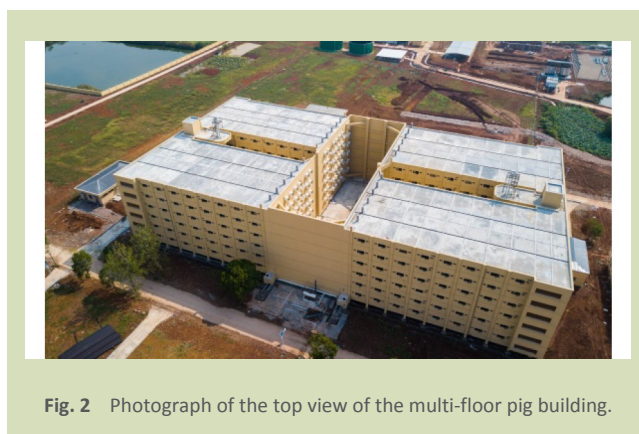


Fig. 2 Photograph of the top view of the multi-floor pig building.

end wall toward the outside and one wet pad was installed at sidewall.

The simplified geometric model of the multi-floor building was shown in Fig. 3. To achieve better simulation, the building was simplified into a cuboid based on the actual dimensions: H_b , L_b and W_b of 21, 118 and 62 m, respectively. The ventilation yard was simplified into an emission surface and the east and west yards were simplified into two cuboids which were subtracted from the whole geometrical model. Since the main objective was to investigate the ammonia dispersion around the building, the inside of the pig house and fans installed in the ventilation yard were not included in the simulation. The six wet pads on the end wall were simplified into two rectangles and the wet pad on the sidewall was simplified into a rectangle. Tunnel ventilation was used in the multi-floor building in summer by using only VX51 fans and wet pads, so the total mass flow rate of the emission outlet was about $2940 \text{ kg}\cdot\text{s}^{-1}$.

The single-floor pig production facility was located in Yan'an, Shaanxi Province, China. The simplified geometrical model of an individual pig house is shown in Fig. 4. Each single-floor building was 48 m long by 25.9 m wide. The ceiling was 2.4 m

high and the roof was 3.6 m high. There were 8 VX51 fans with a ventilation rate of $47,090 \text{ m}^3\cdot\text{h}^{-1}$ in the end wall and the mass flow rate of each fan was $15.3 \text{ kg}\cdot\text{s}^{-1}$. Wet pads were installed on the opposite end wall of fans and two sidewalls. This production facility had 24 identical buildings arranged in two rows at 15 m spacing as shown in Fig. 5. The total floor space was $29,814 \text{ m}^2$ which was more than four times the floor space of the multi-floor building. Fans were installed in the outward-facing end walls and wet pads were on the inward-facing walls.

This single-floor production facility was chosen for comparison with the multi-floor building because the number of pig houses, the internal structure of the pig houses, the number and type of ventilation facilities in the pig houses and the capacity of pigs of the entire single-floor facility were similar to the multi-floor building. Therefore, it was valid to compare the ammonia dispersion from these two facilities.

2.2.2 Meteorological condition and simulation cases

To investigate the effects of different building structures and emission modes on ammonia dispersion, an assumption was made that the single-floor buildings had the same external

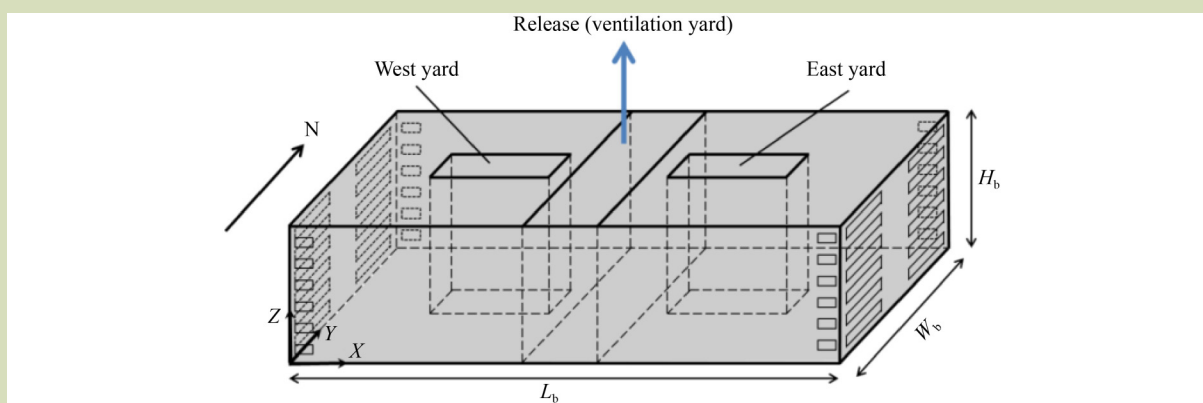


Fig. 3 The geometrical model of the multi-floor pig building.

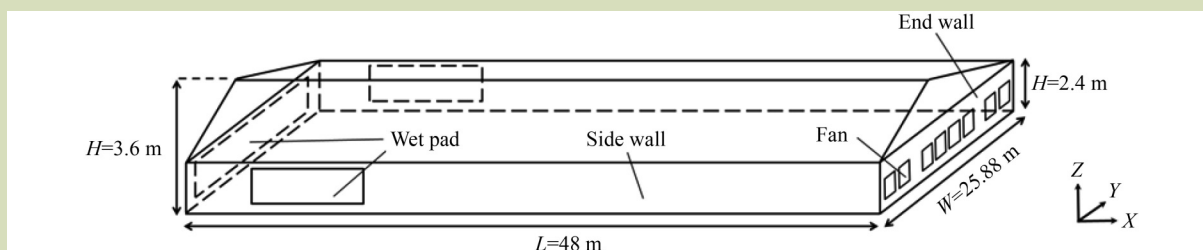


Fig. 4 Simplified geometrical model of an individual single-floor pig building.

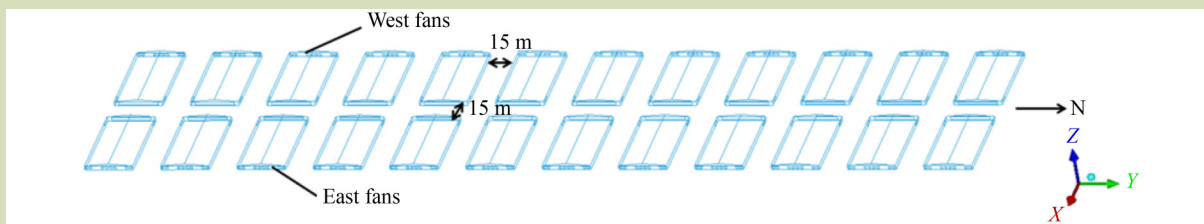


Fig. 5 Arrangement of the single-floor pig buildings in the production facility.

environment as the multi-floor building. According to the measured data of the meteorological condition of Yiwu in 2018, the average temperature is 28.41 °C in summer. The frequency distribution of wind direction and speed in summer were illustrated in Fig. 6 at 10 m aboveground. Regarding the east direction as 0°, the prevailing wind was south-south-east wind (67.5°) with an average velocity of 2 m·s⁻¹ and another

two wind directions with high percentage were south (90°) and south-west (135°). The wind speeds were divided into four numerical ranges and the frequencies of wind speeds in the two ranges of 0–2 and 2–4 m·s⁻¹ were higher.

According to the typical meteorological condition, the included simulation cases are shown in Table 1. The wind speeds chosen were 2, 3 and 5 m·s⁻¹ to compare the ammonia concentration gradients caused by different wind speeds. The wind directions 67.5°, 90° and 135° were chosen according to the frequency. The emission source concentrations were 1, 5, 10, 15 and 20 ppmv which covered a wide range of ammonia concentrations in pig production facilities. A maximum ammonia concentration of 20 ppmv was recommended by the International Commission of Agricultural and Biosystems Engineering^[21]. However, the ammonia concentration in the pig house could be as low as 1 ppmv in summer when instant manure separation technology was used. The simulation cases for the multi- and single-floor buildings were the same.

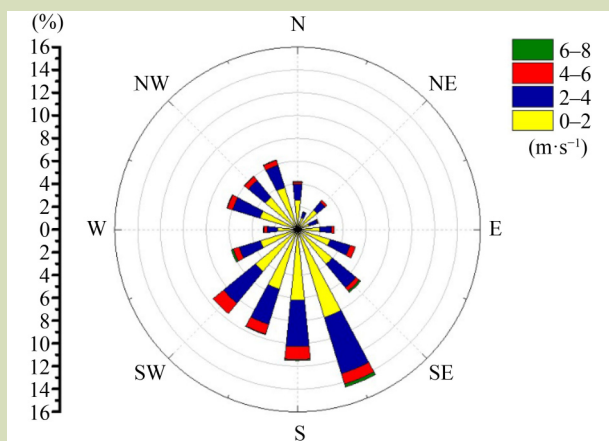


Fig. 6 Wind rose diagram in summer.

2.2.3 Computational domain and mesh

The computational domain was established following the model evaluation guidance^[22]. Given that three wind

Table 1 Simulation cases

Type of pig production facility	Wind direction (°)	Wind speed (m·s ⁻¹)	Emission source concentration (ppmv)
Multi- and single-floor	67.5	2	20
	67.5	3	20
	67.5	5	20
	67.5	2	15
	67.5	2	10
	67.5	2	5
	67.5	2	1
	90	2	20
	135	2	20

directions were used in this study, three computational domains were established. To prevent the influence of boundaries, the distance between building walls and inlet or lateral boundaries should be at least $5H_b$. The outflow boundaries should be at least $15H_b$ away from building walls.

There are residential areas about 1 km away from the multi-floor pig building. To better display the ammonia dispersion,

the computational domain was adjusted according to the simulation. The computational domains of three wind directions of multi-floor building is shown in Fig. 7. The computational domain with $7H_b$ above the building, $5H_b$ between the building walls and the inlet boundaries, $25H_b$ and 1.5 km away from the outlet boundary shown in Fig. 7(a) was for the wind direction of 67.5° . The computational domain with $7H_b$ above the building, $5H_b$ between the building walls,

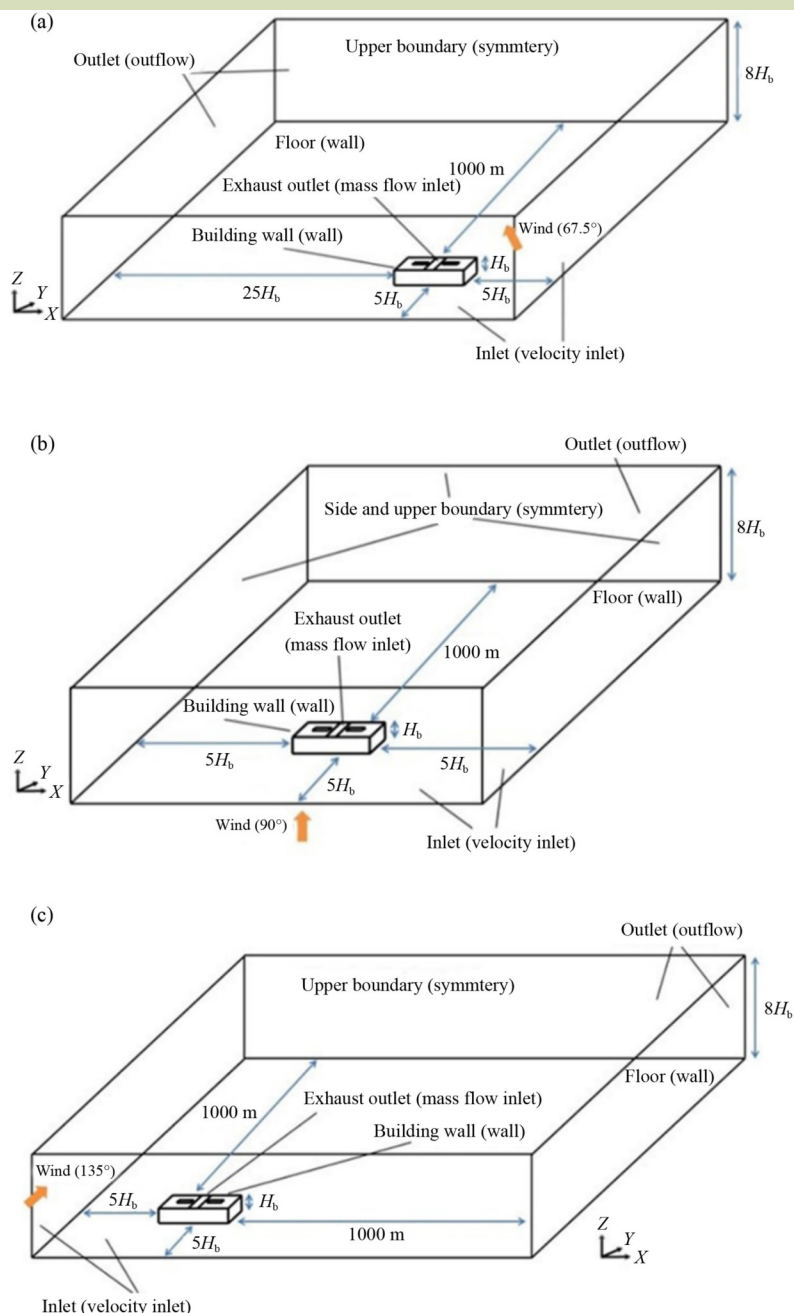


Fig. 7 Computational domains of three different wind directions of the multi-floor pig building: (a) 67.5° ; (b) 90° ; (c) 135° .

and the inlet and lateral boundaries, 1.5 km away from the outlet boundary shown in Fig. 7(b) is for the wind direction of 90°. The computational domain with $7H_b$ above the building, $5H_b$ between the building walls and the inlet boundaries, 1 km away from the outlet boundary shown in Fig. 7(c) is for the wind direction of 135°. The computational domain of the single-floor facility was the same as that of the multi-floor building to avoid the influence of different computational domains.

Based on the experience of grid discretization in the validation simulation, the computational domain of multi- and single-floor buildings were discretized into unstructured tetrahedral grids. Considering the computational domain with the wind direction of 67.5° as an example, the mesh details are shown in Fig. 8.

2.2.4 Boundary conditions and numerical methods

Boundary conditions can greatly influence simulated predictions in wind engineering analysis. The vertical profile of the wind speed at the inlet $U_{in}(z)$ obeys a power law^[23]:

$$\frac{U_{in}(z)}{U_b} = \left(\frac{z}{H_b}\right)^{0.15} \quad (1)$$

where, U_b is the velocity at building height and H_b is building height. The power-law exponent of the vertical profile of the inlet velocity is 0.15 according to the grading of ground roughness.

In addition, the turbulence kinetic energy k and dissipation rate ε at the inlet were computed as:

$$k = \frac{U_*^2}{\sqrt{C_u}} \quad (2)$$

$$\varepsilon = \frac{U_*^3}{K_v(z+z_0)} \quad (3)$$

where, C_u is equal to 0.09, K_v is equal to 0.4, z_0 is surface roughness length, and U_* is friction velocity, which is usually calculated from a specified velocity U_h at a reference height h as:

$$U_* = \frac{K_v U_h}{\ln\left(\frac{h+z_0}{z_0}\right)} \quad (4)$$

A Porous jump boundary is used for wet pads and the pressure change is defined as a combination of Darcy's Law and an additional inertial loss term:

$$\Delta p = \left(\frac{\mu}{\alpha} v + \frac{1}{2} C_2 \rho v^2\right) \Delta m \quad (5)$$

where, μ is the fluid viscosity, α is the permeability of the medium, C_2 is the pressure-jump coefficient, v is the velocity normal to the porous face, and Δm is the thickness of the medium. The Δm of the wet pad of the multi-floor building was 0.15 m. The face permeability, porous medium thickness and pressure-jump coefficient were needed for the setting of porous jump boundary, and the relationship between the pressure drop and velocity was obtained from the experiment results.

As shown in Fig. 7, the outflow boundary was used at the outlet and the mass flow inlet boundary was adopted for the ammonia emission source. A symmetric boundary was used for the top and sides and wall boundary for floors and walls. The

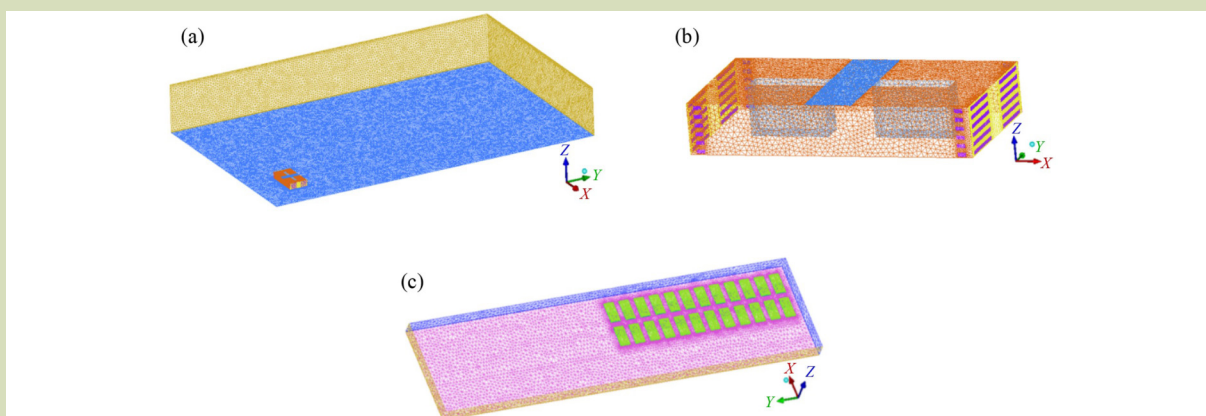


Fig. 8 Grid discretization of three different computational domain of (a) computational domain of the multi-floor pig building; (b) the multi-floor pig building; and (c) computational domain.

boundary conditions of multi- and single-floor building are summarized in Table 2. The three-dimensional simulation of the multi-floor building was based on a finite volume approach for solving the flow and concentration equation. Steady Reynolds-averaged Navier-Stokes method was applied and the realizable $k-\epsilon$ model was used for the turbulence modeling. The scalable wall function was used for all wall boundaries to avoid the deterioration of the calculation results when $Y^+ < 15$ and could give consistent solutions for any refined grid. In addition, the QUICK (Quadratic Upwind Interpolation of the Convective Kinematics) scheme was used for discretizing the convection of momentum and concentration equations. The second order centered difference scheme was used for other terms. Semi-implicit method for pressure linked equations was used for the pressure-velocity correction. Iterations were considered to be in convergence when the residual for the energy equation arrived at 10^{-6} and the residual for other equations reached at 10^{-3} during the simulation. In addition,

the variables also needed to show the tendency to be constant.

3 RESULTS AND DISCUSSION

3.1 Validation

Figure 9 shows the velocity distribution on the roof ($X/H_b = 0$) and behind the cube ($X/H_b = 1$) at the centerline. The experimental data for the validation was provided by Tominaga and Stathopoulos^[24]. According to Fig. 9, the simulation generally agreed with the empirical data. Nevertheless, the negative velocity of the simulation was larger than the experiment in the reverse flow near the ground in Fig. 9(b) and the result was similar to the simulation of Tominaga and Stathopoulos^[24]. The most likely reason is that the $k-\epsilon$ turbulence model cannot reproduce the periodic velocity fluctuation caused by the vortex shedding behind the cube^[25].

Table 2 Boundary conditions of multi- and single-floor pig production facilities

Structure	Conditions
Inlet	Velocity inlet (2, 3 and 5 m·s ⁻¹ at 10 m aboveground; power law at 0.15)
Outlet	Outflow
Exhaust outlet	Mass flow inlet (flow rate 2941 kg·s ⁻¹ of multi-floor building; flow rate 15.3 kg·s ⁻¹ each fan of single-floor buildings)
Side and top	Symmetry
Wet pad	Porous jump
Walls and floors	Non-slip wall, adiabatic

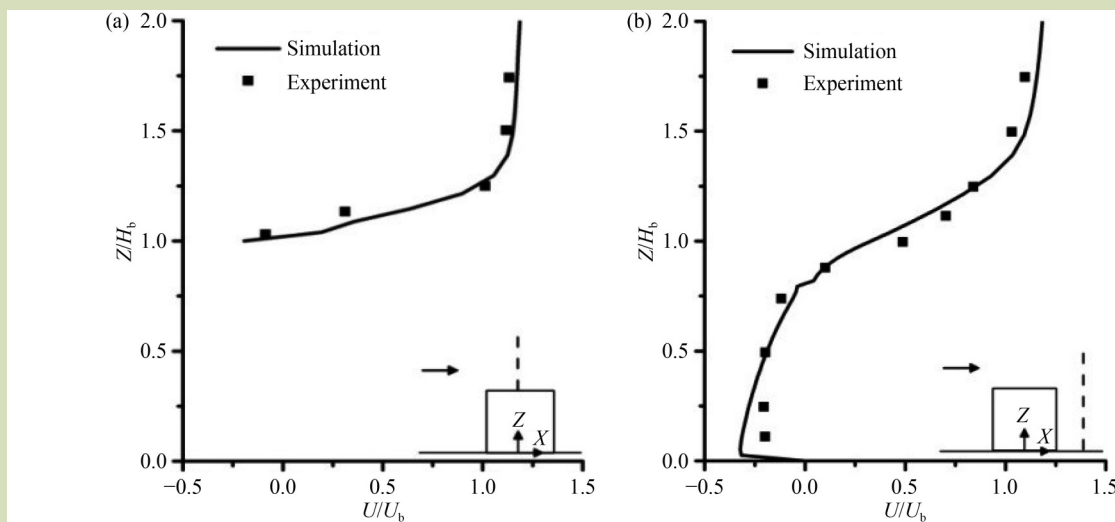


Fig. 9 Simulation and experimental results of velocity: (a) on the roof of the cube ($X/H_b = 0$) at the centerline; (b) behind the cube ($X/H_b = 1$) at the centerline.

Figure 10 showed the simulation and experimental results of dimensionless concentration on the centerline of the roof and leeward wall in streamwise direction^[24]. The dimensionless concentration K was defined as:

$$K = \frac{cH_b^2 U_b}{Q_e} \quad (6)$$

where, c is volumetric fraction of emitted gas and Q_e is flow rate.

According to Fig. 10(a), the simulation could predict pollutant dispersion around the isolated cube. The results showed that the maximum concentration occurred above the vent and the concentration on the leeward wall was greatly reduced because of the sharp edge on the cube. The simulation overestimated the concentration downwind of the vent, including the downwind roof of the vent and leeward wall, in comparison with the experiment. However, the results were similar to the simulation of Tominaga and Stathopoulos^[19]. This is likely due to an over-prediction of the reverse flow behind the cube. The distribution of non-dimensional concentration on the centerline of the roof and sidewall is shown in Fig. 10(b). The simulation underestimated the concentration measured in the experiment on both roof and sidewall. It was observed that the simulated concentration was higher near the ground of the sidewall indicating that the pollutant was transported from the leeward wall by the recirculating airflow, which was the opposite of the experimental situation. Also, the simulation result had a considerable under-prediction of concentration around the edge and this is likely due to an underestimation of the horizontal spread of the pollutant^[19].

In summary, the simulation of velocity and dimensionless concentration were generally in agreement with the

experimental data, which indicated that the simulation method was effective even though the CFD approach was restricted to a neutral stratified atmosphere. This indicated that the pollutant dispersion around a building could be validly predicted using the simulation method applied.

3.2 Comparison of ammonia dispersion from the multi- and single-floor pig buildings

Wind direction of 67.5° , wind speed of $2 \text{ m}\cdot\text{s}^{-1}$ and ammonia emission source concentration of 20 ppmv were used in simulations, and the ammonia concentration gradients of the multi- and single-floor buildings are shown in Fig. 11. The plane of $Z = 1.5 \text{ m}$ used in the simulation was considered as the human inhalation height. The minimum ammonia concentration shown in Fig. 11 was 1.5 ppmv, which is the odor threshold ammonia^[26], thus the areas with ammonia concentration lower than 1.5 ppmv could be considered as unaffected by ammonia.

The simulated highest ammonia concentrations were 7.68 ppmv for the multi-floor pig building (Fig. 11(a)) and 19.3 ppmv for the single-floor facility (Fig. 11(b)), respectively. This was due to the fact that even though the emission source concentration was 20 ppmv, the emission source of multi-floor pig building was 21 m aboveground, so the highest ammonia concentration was only 7.68 ppmv at $Z = 1.5 \text{ m}$ in the west yard. However, the height of the emission source (fan) of the single-floor facility was 0.5 to 1.8 m aboveground, thus the highest ammonia concentration at $Z = 1.5 \text{ m}$ was 19.3 ppmv, close to 20 ppmv near the fan. The ammonia emitted from the multi-floor building apparently dispersed along the direction of wind. The ammonia concentration was higher behind the

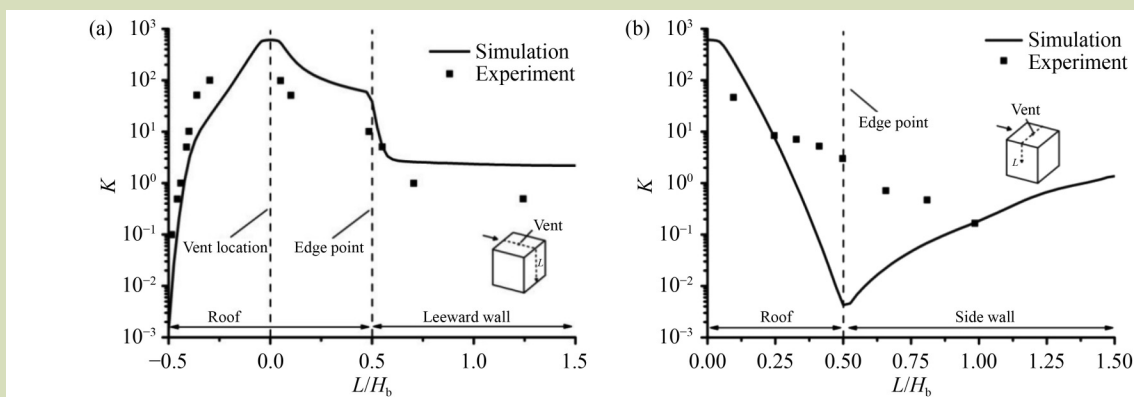


Fig. 10 Validations of dimensionless concentration on: (a) the centerline of the roof and leeward wall in the streamwise direction; (b) the centerline of the roof and sidewall in the lateral direction

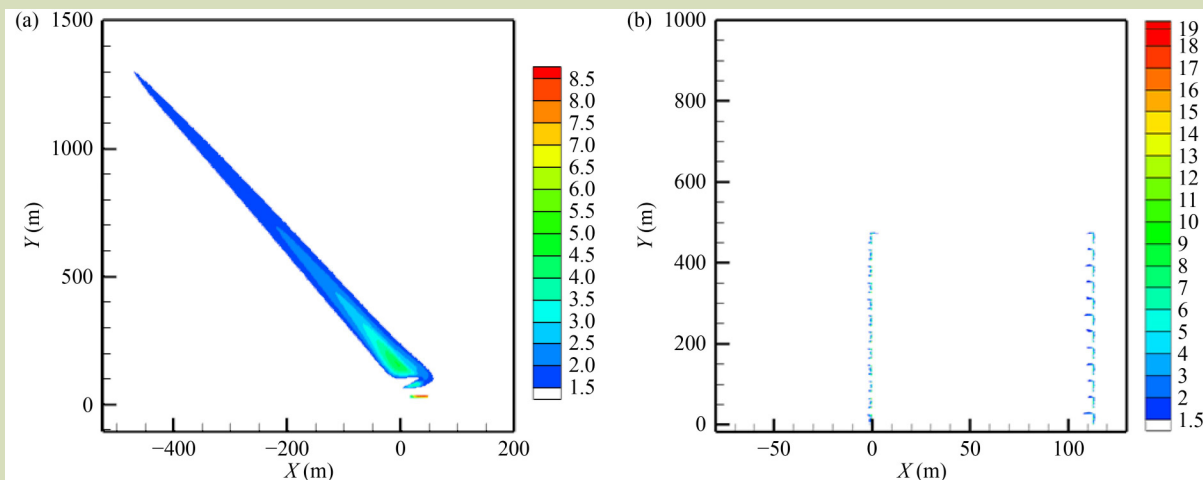


Fig. 11 Ammonia concentration (ppmv) distribution on the plane $Z = 1.5$ m when wind direction was 67.5° , wind speed was $2 \text{ m}\cdot\text{s}^{-1}$ and ammonia concentration of emission source was 20 ppmv: (a) the multi-floor pig building; (b) the flat-floor pig farm.

building which was likely to be due to the reverse airflow under low velocity. In addition, the ammonia concentration was low in the upwind direction from the emission source and the lateral dispersion was not significant in comparison with the dispersion in the direction of the prevailing wind.

For the single-floor facility, the emitted ammonia mainly concentrated near the fans and did not spread as far as from the multi-floor building. However, it still could affect the distance of about 500 m in Y direction (Fig. 11(b)) since the floor space was large and the ammonia concentration around the production facility at $Z = 1.5$ m was high. The detailed local ammonia concentration gradients around the single-floor

facility are shown in Fig. 12. The ammonia emitted from the fans toward the west dispersed only about 2 m and the influence on further distance could be neglected. However, ammonia can disperse into space among adjacent pig buildings with a wind direction of 67.5° , which means that ammonia would disperse in the whole facility. The reason for the great difference of ammonia dispersion between the two types of buildings was that the emission source of multi-floor building was much higher while the concentrated emission flow rate was also much larger, thus the multi-floor building can be seen as an elevated point source with a high emission height, and the ammonia can spread over a long distance. In contrast, the emission sources of the single-floor facility were widely

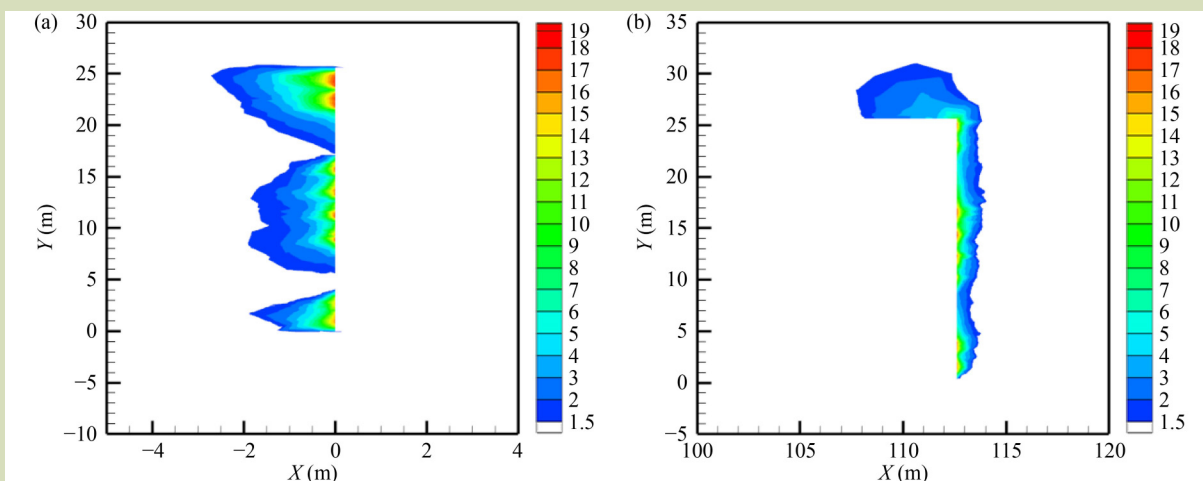


Fig. 12 Local ammonia concentration (ppmv) distributions around fans of the single-floor pig facility: (a) fans toward west; (b) fans toward east.

separated and the flow rate of each emission source was much smaller (about 4% of the multi-floor building), the single-floor facility could be viewed as an area (non-point) source with a low emission height.

In addition to the building height and floor space, the two yards in the multi-floor building were also important contributors to the substantial difference between this building and single-floor facility. The ammonia concentration and velocity vector distribution of multi-floor building at $Y = 31$ m is shown in Fig. 13. As shown in Fig. 13(a), the ammonia concentration in the west yard was higher than in the area around the building, and this means that the ammonia can accumulate in the yard during the operation of the multi-floor building. It is likely that there were vortices in the two yards as shown in Fig. 13(b) such that could not dispersed easily in the wind due to these vortices. It is worth noting that both yards were connected to windows and stairs in the multi-floor building, thus high concentration ammonia in the yards could possibly reenter the building raising ammonia concentrations in the work areas. Therefore, the ammonia accumulation in the yards is a design problem that needs attention.

3.3 Effect of wind direction on ammonia concentration gradient

According to the wind rose diagram in summer, three wind directions of 67.5° , 90° and 135° were chosen for the investigation of wind direction effects, under the wind speed of $2 \text{ m}\cdot\text{s}^{-1}$ and ammonia source concentration of 20 ppmv. Figure 14 shows the ammonia concentration gradients from the multi-floor pig building and the single-floor production facility on the plane $Z = 1.5$ m and the wind directions were 90° and 135° . The case with the wind direction of 67.5° was shown previously in Fig. 11. In Fig. 11 and Fig. 14, it can be seen that ammonia mainly dispersed along the wind direction and the

dispersion distance from the multi-floor pig building was always much larger than that of single-floor facility under investigated wind directions. Also, the highest ammonia concentration in the yards with a wind direction of 135° was 10.8 ppmv, which was higher than 7.68 ppmv with a wind direction of 67.5° and 4.79 ppmv with a wind direction of 90° . For the single-floor facility, the effect of wind direction on ammonia concentration dispersal was not significant.

3.4 Effect of wind speed on ammonia concentration gradient

The average wind speed of $2 \text{ m}\cdot\text{s}^{-1}$ was used as a typical value in previous sections, but different wind speeds could also affect ammonia dispersal. The ammonia concentrations at selected locations (Fig. 15) around the multi- and single-floor buildings at $Z = 1.5$ m with wind speeds of 2, 3 and $5 \text{ m}\cdot\text{s}^{-1}$ were estimated for with a wind direction of 67.5° and emission source concentration of 20 ppmv. For the multi-floor building, the five location points selected in this investigation are shown in Fig. 15(a). Point 1 was located in the middle of the west yard, and Points 2–5 were located along the wind direction of 67.5° . As shown in Fig. 16(a), the ammonia concentration at Point 1 was much higher than other points, which was consistent with Fig. 11. However, the ammonia concentration in the west yard increased with the increased wind velocity. This means that higher wind speed is the likely cause of greater ammonia accumulation in the yard. It is important to note that with the increase of wind speed from 3 to $5 \text{ m}\cdot\text{s}^{-1}$, the increased accumulation of ammonia was much less compared to that when wind speed was increased from 2 to $3 \text{ m}\cdot\text{s}^{-1}$. This indicated that the effect of wind speed on ammonia accumulation was limited when the emission source concentration was constant. In contrast, ammonia concentrations at Points 2–5 were slightly less with higher wind speed, suggesting a dilution effect at high wind speed.

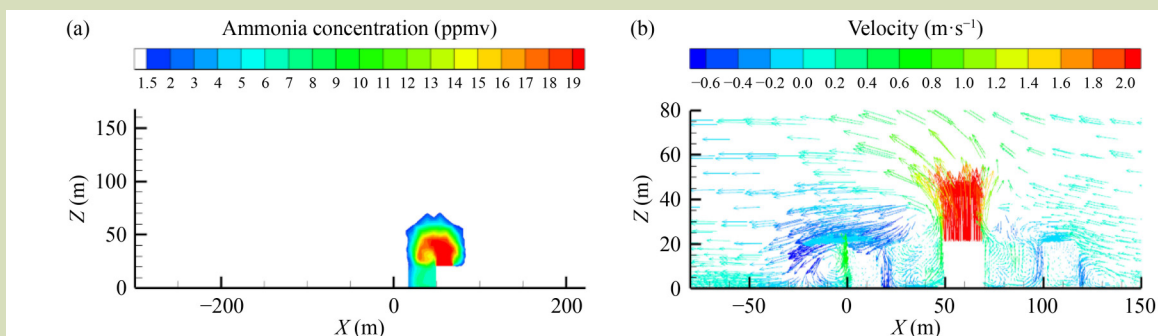


Fig. 13 Plane $Y = 31$ m of the multi-floor pig building: (a) ammonia concentration distribution; (b) velocity vector distribution.

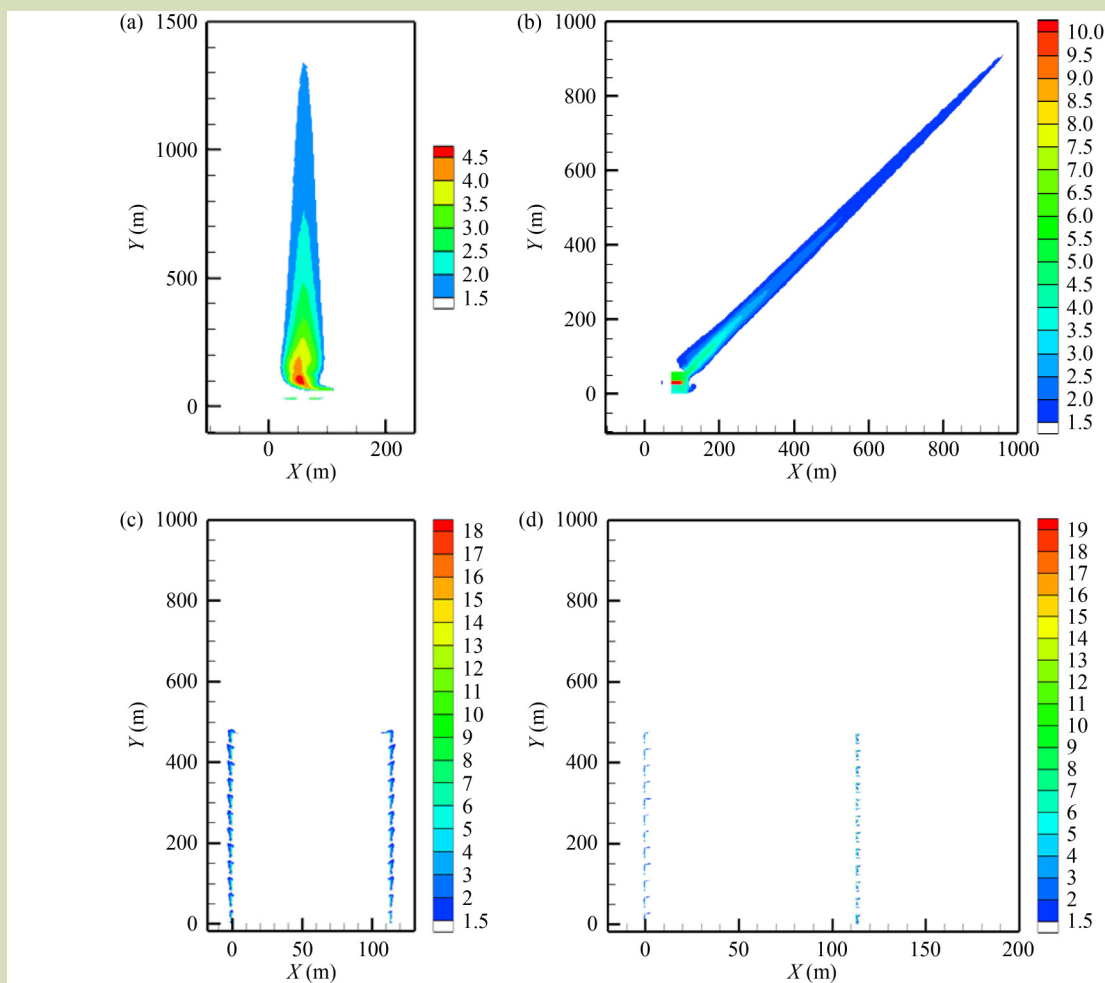


Fig. 14 Ammonia concentration gradient (ppmv) on the plane $Z = 1.5$ m under different wind directions, wind speed of $2 \text{ m}\cdot\text{s}^{-1}$ and emission source concentration of 20 ppmv: (a) 90° , the multi-floor pig building; (b) 135° , the multi-floor pig building; (c) 90° , the flat-floor pig farm; (d) 135° , the flat-floor pig farm.

For the single-floor facility, six points were selected in the computational domain as shown in Fig. 15(b). Point 1 was on the east side of east fans and Point 2 was in the middle of the two rows of buildings. Points 3–5 were on the dispersion path of west fans under the wind direction of 67.5° . As shown in Fig. 16(b), the ammonia concentration at Point 1 was much lower than other points because it was upwind and ammonia could not disperse easily to this point. The ammonia concentration at Point 2 was the highest, suggesting that ammonia might accumulate in the single-floor facility. However, the highest ammonia concentration was only 0.118 ppmv, which was lower than the odor threshold for ammonia, thus this accumulation would not significantly influence the environment. For Points 3–6, the ammonia concentration decreased with the increased wind speed.

As shown in Fig. 16, the effects of different wind speeds on the ammonia dispersion outside the two types of pig facilities had similar trends but at differing concentrations. In addition, different wind speeds can affect the ammonia accumulation in the yards of the multi-floor building and in the space between individual buildings in the single-floor facility. Therefore, local wind speed should be taken into account during site selection for intensive pig production facilities considering emissions accumulation and dispersion distance.

3.5 Effect of source concentration level on ammonia concentration gradient

The emission source concentration is not only related to breeding and operation management with a pig production facility but also depends on waste gas treatment. The different

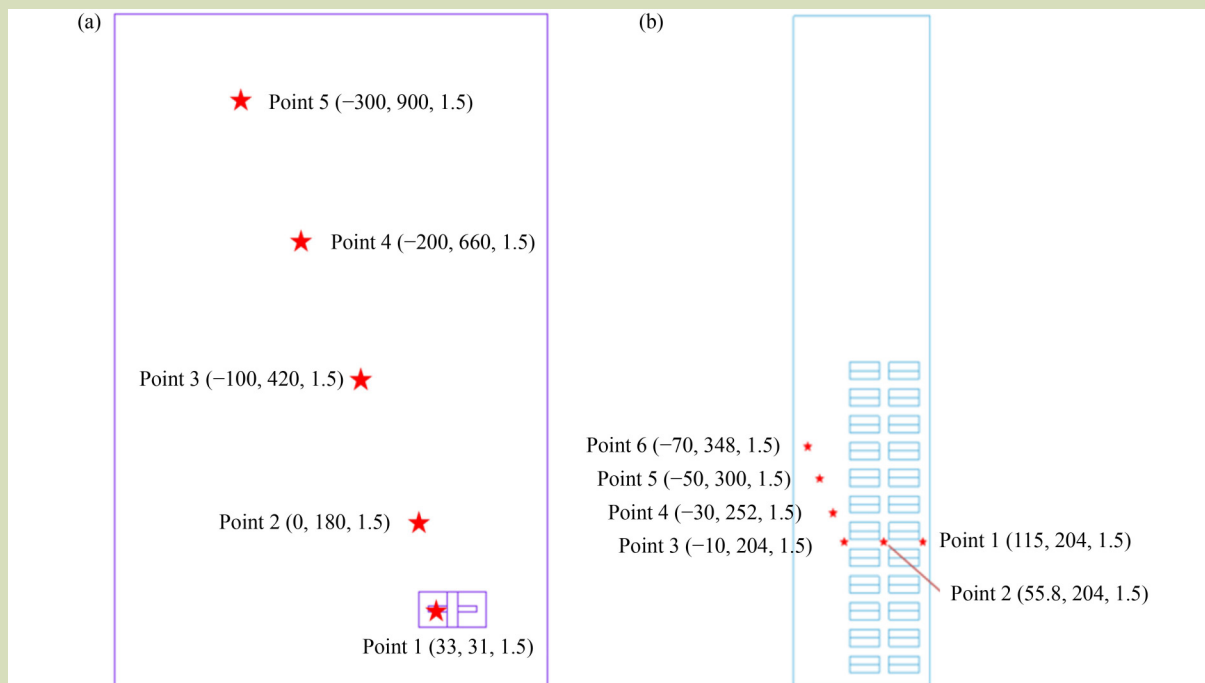


Fig. 15 Points selected to compare the ammonia concentrations at different wind speeds (as shown in Fig. 16): (a) the multi-floor pig building; (b) the flat-floor pig farm.

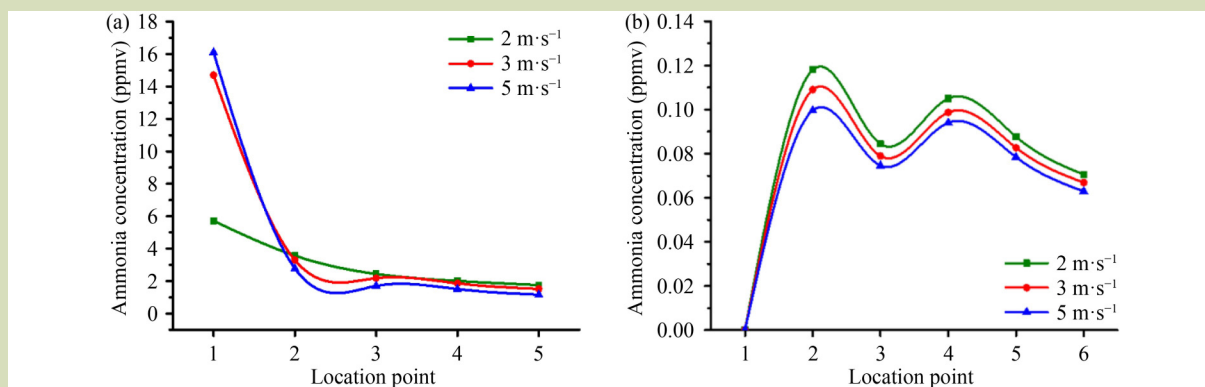


Fig. 16 Ammonia concentrations on the plane $Z = 1.5$ m with wind speeds of $2 \text{ m}\cdot\text{s}^{-1}$, $3 \text{ m}\cdot\text{s}^{-1}$ and $5 \text{ m}\cdot\text{s}^{-1}$, the wind direction of 67.5° and the emission source concentration of 20 ppmv at points as detailed in Fig. 15: (a) the multi-floor pig building; (b) the flat-floor pig farm.

source concentrations were set to 1, 5, 10, 15 and 20 ppmv in order to cover a meaningful range of possibilities with wind direction of 67.5° and speed of $2 \text{ m}\cdot\text{s}^{-1}$. The ammonia concentration gradients from the multi- and single-floor facilities at $Z = 1.5$ m under different source concentrations are shown in Fig. 17 (for the points specified in Fig. 15). The ammonia concentration dispersal increased with the increase of emission source concentration at all points. The differences between the points were larger when the emission source

concentration was higher. Therefore, the emission source concentration is an important factor to consider in layout and site selection of such facilities especially near residential areas.

3.6 Ammonia dispersion distance of multi-floor pig building

In this study, the dispersion distance was defined as the maximum distance ammonia of dispersal outside of pig

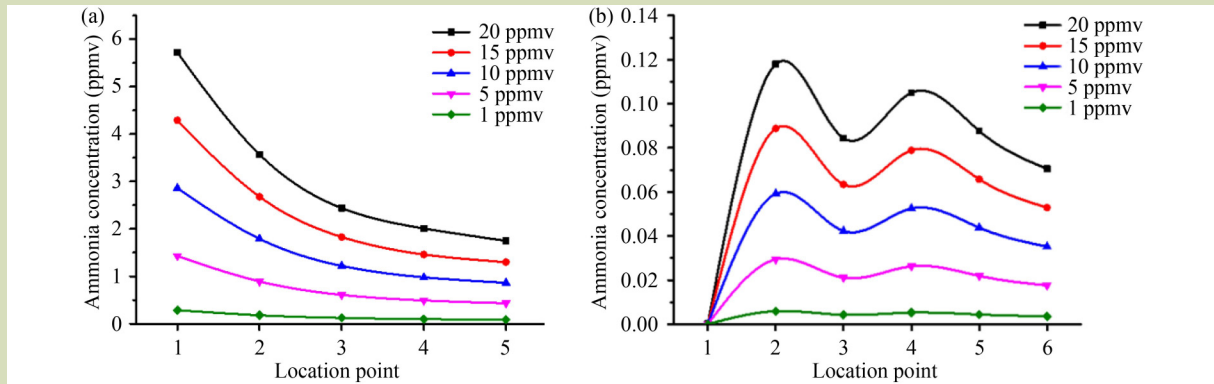


Fig. 17 Ammonia concentration gradients on the plane $Z = 1.5$ m under emission source concentrations of 1, 5, 10, 15 and 20 ppmv with the wind direction of 67.5° and speed of $2 \text{ m}\cdot\text{s}^{-1}$ at points as detailed in Fig. 15: (a) the multi-floor pig building; (b) the flat-floor pig farm.

building where the ammonia concentration was reduced to the odor threshold concentration (1.5 ppmv). According to the results above, the ammonia dispersion distance from the multi-floor building was much further than from the single-floor facility. Therefore, the dispersion distance from the multi-floor building under different wind directions, wind speeds and emission source concentrations summarized in Table 3. The purpose is to compare the influence of different parameters on the ammonia dispersion distance of the multi-floor pig building and surrounding environment, and thereby to provide references for the site selection.

Firstly, the results from Table 3 showed that with the wind speed of $2 \text{ m}\cdot\text{s}^{-1}$ the dispersion distance with a wind direction of 67.5° was 1.38 km, which was the furthest of the three wind directions. Nevertheless, the dispersion distances with wind directions of 90° and 135° were 1.35 and 1.32 km, respectively, which were only slightly shorter compared to 1.38 km. This indicated that the wind direction had no significant impact on the dispersion distance when the wind speed and emission

source concentration were the same. Secondly, the ammonia dispersion distance decreased markedly with the decrease of emission source concentration. Specifically, the dispersion distance decreased from 1.38 to 0.73 km when the emission source concentration decreased from 20 to 15 ppmv, indicating that the reduction of emission source concentration could effectively reduce the dispersion distance. The further decrease of source concentration can efficiently reduce the dispersion distance (Table 3). These results indicate that for multi-floor buildings, it is important to control the emission source concentration to about 15 ppmv in order to minimize the impact on surrounding residents. Thirdly, the dispersion distance decreased with the increase of wind speed. When the wind speed was below $3 \text{ m}\cdot\text{s}^{-1}$, the dispersion distance was more than 1 km. The average surface wind speed in summer in China is about $2\text{--}2.5 \text{ m}\cdot\text{s}^{-1}$. Therefore, the multi-floor pig building should be built about 1.4 km away from the residential areas, if the emission source concentration was controlled under 20 ppmv to ensure that ammonia would not affect the surrounding residents.

Table 3 Ammonia dispersion distance under different wind directions, wind speeds and emission source concentrations

Case	Wind direction ($^\circ$)	Wind speed ($\text{m}\cdot\text{s}^{-1}$)	Emission source concentration (ppmv)	Dispersion distance (m)
1	67.5	2	20	1380
2	67.5	3	20	1043
3	67.5	5	20	684
4	67.5	2	15	727
5	67.5	2	10	320
6	67.5	2	5	41 (in the yard)
7	90	2	20	1345
8	135	2	20	1324

4 CONCLUSIONS

In this study, three-dimensional CFD simulations based on the actual dimensions of multi- and single-floor facilities were conducted to investigate the difference in ammonia dispersion between such facilities. The results showed that the ammonia dispersion distance of multi-floor building was much greater than for single-floor facilities at $Z = 1.5$ m and that the ammonia can accumulate in the yards of multi-floor buildings. Under different wind directions, ammonia always dispersed along the dominant wind direction, but the influence of wind

direction on the dispersion distance was not significant. The ammonia concentration and dispersion distance decreased with the increase of wind speed but higher wind speeds were more likely to lead to ammonia accumulation in yards. The ammonia concentration and dispersion distance decreased markedly with the decrease of emission source concentration, and the reduction of emission source concentration could therefore substantially reduce the dispersion distance. If the ammonia source concentration was controlled to under 20 ppmv, then multi-floor pig production buildings should be located at least 1.4 km away from residential areas to ensure that the local residents were not impacted by ammonia odors.

Acknowledgements

The research was financially supported by the National Key R&D Program of China (2022YFE0115600) and the Key Research and Development Program of Zhejiang Province (2022C02045).

Compliance with ethics guidelines

Yicong Xin, Li Rong, Gunther Schaubberger, Dejie Liu, Xiusong Li, Zhihua Yang, Songming Zhu, and Dezhao Liu declare that they have no conflicts of interest or financial conflicts to disclose. This article does not contain any studies with human or animal subjects performed by any of the authors.

REFERENCES

- Du L, Yang C, Dominy R, Yang L, Hu C, Du H, Li Q, Yu C, Xie L, Jiang X. Computational fluid dynamics aided investigation and optimization of a tunnel ventilated poultry house in China. *Computers and Electronics in Agriculture*, 2019, **159**: 1–15
- Hu Y, Cheng H, Tao S. Environmental and human health challenges of industrial livestock and poultry farming in China and their mitigation. *Environment International*, 2017, **107**: 111–130
- Saha C K, Zhang G, Kai P, Bjerg B. Effects of a partial pit ventilation system on indoor air quality and ammonia emission from a fattening pig room. *Biosystems Engineering*, 2010, **105**(3): 279–287
- Rebolledo B, Gil A, Pallarés J. A spatial ammonia emission inventory for pig farming. *Atmospheric Environment*, 2013, **64**: 125–131
- Smit L A M, Heederik D. Impacts of intensive livestock production on human health in densely populated regions. *GeoHealth*, 2017, **1**(7): 272–277
- Benincà E, van Boven M, Hagensnaars T, van der Hoek W. Space-time analysis of pneumonia hospitalisations in the Netherlands. *PLoS One*, 2017, **12**(7): e0180797
- Pohl H R, Citra M, Abadin H A, Szadkowska-Stańczyk I, Kozajda A, Ingerman L, Nguyen A, Murray H E. Modeling emissions from CAFO poultry farms in Poland and evaluating potential risk to surrounding populations. *Regulatory Toxicology and Pharmacology*, 2017, **84**: 18–25
- Zilio M, Orzi V, Chiodini M E, Riva C, Acutis M, Boccasile G, Adani F. Evaluation of ammonia and odour emissions from animal slurry and digestate storage in the Po Valley (Italy). *Waste Management*, 2020, **103**: 296–304
- Lateb M, Meroney R N, Yataghene M, Fellouah H, Saleh F, Boufadel M C. On the use of numerical modelling for near-field pollutant dispersion in urban environments—A review. *Environmental Pollution*, 2016, **208**(Pt A): 271–283
- Allegrini J, Dorer V, Carmeliet J. Coupled CFD, radiation and building energy model for studying heat fluxes in an urban environment with generic building configurations. *Sustainable Cities and Society*, 2015, **19**: 385–394
- Blocken B, Stathopoulos T, Carmeliet J, Hensen J L M. Application of computational fluid dynamics in building performance simulation for the outdoor environment: an overview. *Journal of Building Performance Simulation*, 2011, **4**(2): 157–184
- Botham-Myint D, Recktenwald G W, Sailor D J. Thermal footprint effect of rooftop urban cooling strategies. *Urban Climate*, 2015, **14**: 268–277
- Skelhorn C, Lindley S, Levermore G. The impact of vegetation types on air and surface temperatures in a temperate city: a fine scale assessment in Manchester, UK. *Landscape and Urban Planning*, 2014, **121**: 129–140

14. Yang X, Zhao L, Bruse M, Meng Q. Evaluation of a microclimate model for predicting the thermal behavior of different ground surfaces. *Building and Environment*, 2013, **60**: 93–104
15. Gu Z L, Zhang Y W, Lei K B. Large eddy simulation of flow in a street canyon with tree planting under various atmospheric instability conditions. *Science China. Technological Sciences*, 2010, **53**(7): 1928–1937
16. Tan Z, Dong J, Xiao Y, Tu J. A numerical study of diurnally varying surface temperature on flow patterns and pollutant dispersion in street canyons. *Atmospheric Environment*, 2015, **104**: 217–227
17. Olivardia F G G, Zhang Q, Matsuo T, Shimadera H, Kondo A. Analysis of pollutant dispersion in a realistic urban street canyon using coupled CFD and chemical reaction modeling. *Atmosphere*, 2019, **10**(9): 479
18. Ntinis G K, Shen X, Wang Y, Zhang G. Evaluation of CFD turbulence models for simulating external airflow around varied building roof with wind tunnel experiment. *Building Simulation*, 2018, **11**(1): 115–123
19. Tominaga Y, Stathopoulos T. Numerical simulation of dispersion around an isolated cubic building: comparison of various types of k - ϵ models. *Atmospheric Environment*, 2009, **43**(20): 3200–3210
20. Li W W, Meroney R N. Gas dispersion near a cubical model building. Part I. Mean concentration measurements. *Journal of Wind Engineering and Industrial Aerodynamics*, 1983, **12**(1): 15–33
21. Rodriguez M R, Losada E, Besteiro R, Arango T, Velo R, Ortega J A, Fernandez M D. Evolution of NH_3 concentrations in weaner pig buildings based on setpoint temperature. *Agronomy*, 2020, **10**(1): 107
22. Franke J, Hellsten A, Schlunzen K H, Carissimo B. The COST 732 Best Practice Guideline for CFD simulation of flows in the urban environment: a summary. *International Journal of Environment and Pollution*, 2011, **44**(1–4): 419–427
23. Richards P J, Hoxey R P. Appropriate boundary conditions for computational wind engineering models using the k - ϵ turbulence model. *Journal of Wind Engineering and Industrial Aerodynamics*, 1993, **46–47**: 145–153
24. Tominaga Y, Stathopoulos T. Numerical simulation of dispersion around an isolated cubic building: model evaluation of RANS and LES. *Building and Environment*, 2010, **45**(10): 2231–2239
25. Bazdidi-Tehrani F, Jadidi M. Large eddy simulation of dispersion around an isolated cubic building: evaluation of localized dynamic k_{SGS} -equation sub-grid scale model. *Environmental Fluid Mechanics*, 2014, **14**(3): 565–589
26. Hanajima D, Kuroda K, Morishita K, Fujita J, Maeda K, Morioka R. Key odor components responsible for the impact on olfactory sense during swine feces composting. *Bioresource Technology*, 2010, **101**(7): 2306–2310